Ferromagnetism in $Al_{1-x}Cr_xN$ thin films by density functional calculations

Q. Wang, A. K. Kandalam, Q. Sun, and P. Jena
Physics Department, Virginia Commonwealth University, Richmond, Virginia 23284, USA
(Received 16 September 2005; revised manuscript received 26 January 2006; published 14 March 2006)

We report the results of a theoretical study of magnetic coupling between Cr atoms doped in bulk AlN as well as AlN $(11\bar{2}0)$ thin films having wurtzite structure. The calculations are based on density fuctional theory with the generalized gradient approximation to the exchange and correlation potential. In the thin film, modeled by a slab of finite thickness, Cr atoms are found to cluster around N on the surface layer and couple ferromagnetically. The results for the Cr-doped AlN crystal are similar, namely, Cr atoms cluster around N and couple ferromagnetically. In the thin film, the preference of Cr to occupy surface sites over the bulk sites is shown to be due to reduced coordination of the surface atoms. As the distance between the Cr atoms increases, both the ferro- and antiferromagnetic states become energetically degenerate and this degeneracy may account for the observed low magnetic moment per Cr atom.

DOI: 10.1103/PhysRevB.73.115411 PACS number(s): 61.46.−w, 75.50.Pp, 36.40.Cg

I. INTRODUCTION

The study of dilute magnetic semiconductor (DMS) materials has been a topic of great interest in the past decade since it was realized that the spin degree of freedom of electrons can be exploited in the manufacturing of spintronic devices. Numerous experiments have been carried out to search for DMS materials that can be ferromagnetic at room temperatures by doping transition metal elements into several wide-band-gap semiconductors. While ferromagnetism has been confirmed in materials such as (In,Mn)As and (Ga,Mn)As, those with room-temperature ferromagnetism such as Mn-doped GaN and ZnO have been controversial.

One of the systems that has received particular attention in recent years involves Cr-doped AlN. Using a variety of experimental techniques[1–4] such as reactive sputtering, reactive molecular beam epitaxy, and metalorganic chemical vapor deposition, Cr-doped AlN thin films have been synthesized and are found to exhibit ferromagnetic properties at room temperature. The saturation magnetic moment per atom, however, has been found to be small and vary from $0.45\mu_B$/atom to $1.0\mu_B$/atom. In some experiments[5] Cr-doped AlN thin film has been found to exhibit ferromagnetism up to 900 K. In a recent study Polyakov *et al.*[6] have shown that samples containing 2 at. % of Cr-doped AlN are ferromagnetic. In addition, the authors have pointed out that only 10% of the Cr atoms contributed to the observed ferromagnetism.

There are very few theoretical studies available on Cr-doped AlN. Of the two recent calculations[2,7] that we are aware of, the authors have studied Cr-doped bulk AlN while the experiments have been performed on AlN thin films. The calculations show that Cr atoms couple ferromagnetically but the magnetic moment per Cr atom is $3.0\mu_B$, which is much larger than the experimental value. No explanation exists to account for this discrepancy nor has any attempt been made to find the preferred sites Cr atoms occupy. For example, do Cr atoms prefer to occupy surface, subsurface, or bulk sites? Do Cr atoms form clusters by residing at nearest-neighbor sites or do they prefer to stay at large distances from each other? Does the magnetic moment at the Cr site depend on the sites Cr atoms occupy?

In this paper we present a theoretical study that addresses these issues. By modeling the AlN thin film by a slab of nine layers we have determined the preferential site of Cr (i.e., surface versus bulk), the relative stability of ferromagnetic (FM) and antiferromagnetic (AFM) configurations, and the magnetic moment as a function of concentration. Results for Cr-doped bulk AlN are also presented here so that they can be compared not only with earlier theoretical studies[2,7] on bulk AlN but also with the present results on thin films. We show that Cr atoms prefer to cluster around N atoms and the FM state is energetically more favorable than the AFM state in both bulk and thin films, which is in agreement with the experiments. However, as the distance between the Cr atoms increases, the FM and AFM states become energetically degenerate in both bulk and thin films. Hence, the possibility of the existence of these two types of magnetic states at low concentrations can explain the observed low saturation magnetization. Also, the magnetic moment on Cr atoms is found to be insensitive to the site preference of Cr. In the following Sec. II we provide a brief outline of our computational procedure. Our results are presented and discussed in Sec. III.

II. THEORETICAL APPROACH

The AlN thin film was modeled by a 2×2 nine-layer slab having wurtzite structure along the $[11\bar{2}0]$ surface direction. The slab supercell contains a total of 144 atoms ($Al_{72}N_{72}$) (see Fig. 1). A vacuum region of 10 Å separated the slabs from one another along the $[11\bar{2}0]$ direction. To preserve symmetry, the top and bottom layers of the slab were taken to be identical. The central five layers are kept frozen in their bulk positions, while the atoms in the top and bottom two layers of the slab are allowed to relax without any symmetry constraint. The slab extends to infinity along the [0001] and $[1\bar{1}00]$ directions through the periodic repetition of a supercell to mimic a real surface situation. To study the magnetic coupling between Cr atoms and the preferred distance be-

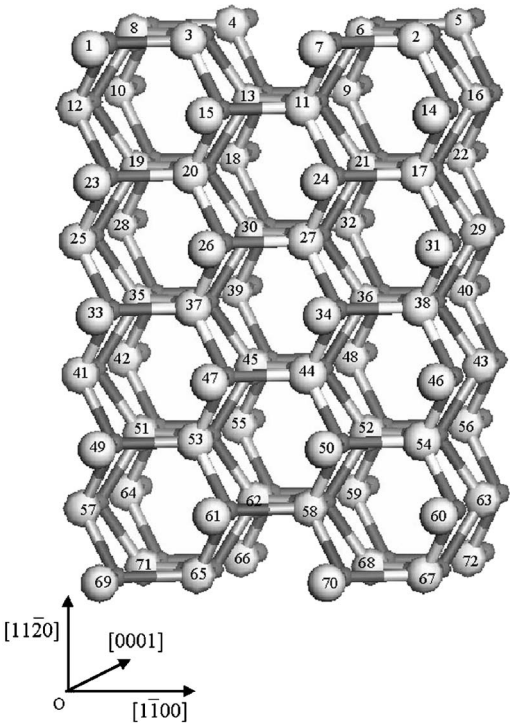

FIG. 1. The schematic representation of a nine-layer slab model for wurtzite AlN (11$\bar{2}$0) surface, which consists of 72 Al and 72 N atoms. The lighter and numbered spheres are Al, the darker and smaller spheres are N atoms.

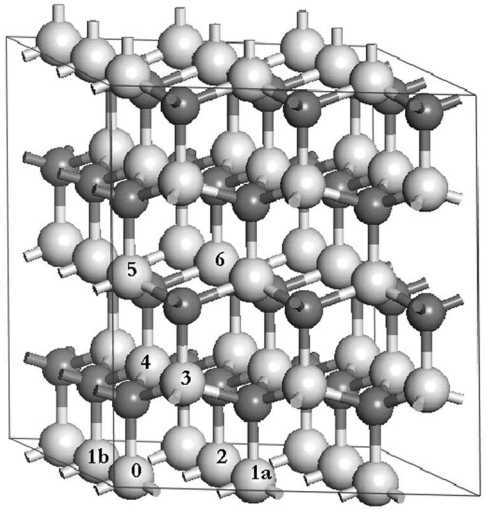

FIG. 2. The schematic representation of a wurtzite AlN ($3\times3\times3$) supercell, which contains 36 Al and 36 N atoms. The lighter and larger spheres are Al, the darker and smaller spheres are N atoms. In the supercell the directions through atoms 0 and 1a, 0 and 1b, and 0 and 5 correspond to [10$\bar{1}$0], [01$\bar{1}$0], and [0001], respectively.

tween them, we have replaced two Al atoms with two Cr atoms at different sites. The calculations of total energies, forces, and optimization of geometries were carried out using density functional theory and the Perdew-Wang 1991 (PW91) functional[8] for the generalized gradient approximation for the exchange and correlation potential. A plane-wave basis set with projector-augmented wave potentials[9,10] for Al, N, and Cr as implemented in the Vienna *ab initio* simulation package (VASP)[11] was employed. The energy cutoff in all these calculations was set to 300 eV, whereas the convergence in energy and force were set to 10^{-4} eV and 10^{-3} eV/Å, respectively. The *k*-point convergence was attained with a $6\times5\times1$ Monkhorst-Pack grid[12] and tests with up to $6\times6\times2$ *k*-point meshes were also made. For the nine-layer slab to be a good representation of the thin film the interactions between the top and bottom surfaces of the slab must be negligible and the results must converge. To test the accuracy of our model in mimicking the thin film, we have studied the sensitivity of our results by varying the number of layers in the undoped slab. We have tested for these factors by carrying out surface relaxation calculations on undoped 1×2 AlN (11$\bar{2}$0) slabs containing five, seven, nine, and eleven layers corresponding to 40, 56, 72, and 88 atoms/supercell, respectively. The distances between the topmost and bottom-most layers in five-, seven-, nine-, and eleven-layer slabs are 6.224, 9.336, 12.448, and 15.560 Å, respectively. The changes in the Al-N bond lengths and energy gain due to the surface relaxation were found to converge well in the seven-layer slab. However, in order to model low Cr doping concentrations in the AlN thin film, we used a 2×2 nine-layer slab. This larger slab is adequate to model the thin film as well as to mimic low dopant concentrations.

We have also performed calculations on the bulk wurtzite structure of AlN which can be compared with earlier bulk calculations and our present thin film results. For the bulk calculation, a $3\times3\times2$ $Al_{36}N_{36}$ supercell, as shown in Fig. 2, was used. Here, two Al atoms were replaced with two Cr atoms to study their magnetic coupling. The Cr-Cr distance inside the supercell was varied by changing the replaced Al sites, until the total energy reached a minimum. The *k*-point convergence was achieved with a $4\times4\times4$ Monkhorst-Pack *k*-point mesh.

III. RESULTS

We first present our results on bulk Cr-doped AlN. To study the magnetic coupling between Cr atoms in the AlN supercell, we need to replace at least two Al atoms with two Cr atoms. Thus an $Al_{34}Cr_2N_{36}$ supercell with a 5.56% Cr doping concentration has been generated. There are many possible sites for Cr atoms to reside. Following our previous works[13,14] to simulate different Cr-Cr and Cr-N distances as well as Cr-N-Cr bond angles, we have tried seven different configurations by varying the sites of Cr atoms in the $Al_{34}Cr_2N_{36}$ supercell. The total energies corresponding to both FM and AFM spin alignments were calculated for all these configurations to determine the preferred magnetic ground state. The calculations of magnetic moments located at each Cr site were also carried out self-consistently. It was found that the configuration corresponding to the replacement of Al at sites (0,1a) in Fig. 2 is equivalent to that at sites (0,1b). That is to say that [10$\bar{1}$0] and [01$\bar{1}$0] directions are isotropic as expected. Therefore, the results for only six

TABLE I. The energy difference ΔE_0 (ΔE) between AFM and FM states ($\Delta E = E_{AFM} - E_{FM}$, in eV), the relative energy $\Delta\epsilon_0$ ($\Delta\epsilon$) (in eV) calculated with respect to the ground-state configuration II (configuration I) without (with) geometry optimization, and the optimized Cr-C and the nearest Cr-N distances (in Å) for bulk $Al_{34}Cr_2N_{36}$ supercell. First column identifies the Al sites in Fig. 1 that are replaced by Cr.

Configurations	ΔE_0	$\Delta\varepsilon_0$	ΔE	$\Delta\varepsilon$	Coupling	$d_{Cr\text{-}Cr}$	$d_{Cr\text{-}N}$
I (0, 1)	0.236	0.001	0.332	0.000	FM	3.010	1.891
II (0, 2)	0.236	0.000	0.323	0.011	FM	3.017	1.891
III (0, 3)	0.214	0.487	0.129	0.271	FM	2.994	1.903
IV (0, 4)	0.022	0.647	−0.060	0.636	AFM	4.399	1.970
V (0, 5)	0.040	0.637	−0.023	0.571	AFM	5.013	1.963
VI (0, 6)	0.038	0.710	−0.012	0.701	AFM	5.913	1.970

configurations are summarized in Table I. In the first column, we specified the Al atoms that were replaced by Cr (see Fig. 2). The energy difference ΔE between the AFM and FM-states for all these configurations with and without full geometry optimization is listed in columns 4 and 2, respectively. The relative energy $\Delta\varepsilon$ with respect to the ground state with and without geometry optimization is tabulated in the fifth and third columns, respectively. We also listed the optimized distance between Cr and Cr and that between the nearest Cr and N in the last two columns of this table. It was found that configurations I and II are energetically degenerate and Cr atoms prefer to cluster around N atoms for both unrelaxed and relaxed cases. When the supercell was not allowed to relax, it was found that configuration II is the ground-state and the FM state is more stable compared to the corresponding AFM state in all these configurations. In the ground-state configuration, the FM state is 0.236 eV lower in energy than the AFM state. When the structure was allowed to relax without any symmetry constraint, the FM state still remained as the ground state but configuration II was found to be lying higher in energy than configuration I by 0.011 eV. The ground state, configuration I, has the energy of the FM state being 0.332 eV lower than that of the AFM state. The total magnetic moment of this system is found to be $6.00\mu_B$, while the moment located on each of the Cr atom is $2.583\mu_B$ and mainly comes from the Cr $3d$ orbital ($2.510\mu_B$) with small contributions arising from Cr $4s$ ($0.05\mu_B$) and $4p$ ($0.02\mu_B$). In Fig. 3 we plot the energy difference ΔE and the magnetic moments on Cr for all the six configurations. The magnetic moments at the Cr sites in the FM state (configurations I, II, and III) and the AFM state (configurations IV, V, and VI) range from $2.46\mu_B$ to $2.66\mu_B$, which is similar to the magnetic moment distribution in Cr-doped GaN.[15] The results are in agreement with previous theoretical calculations on Cr-doped bulk AlN.[2,7]

We now present our results on Cr-doped AlN thin films. First, we discuss the surface reconstruction of an undoped AlN $(11\bar{2}0)$ thin film modeled by a nine-layer slab. Relaxation of surface and subsurface layers on either side of the slab resulted in a total energy gain of 5.261 eV. Assuming that this energy gain is shared among the atoms that have been relaxed, we find the energy gain per Al-N dimer to be 0.164 eV. Due to the relaxation, surface Al atoms are displaced inward by about −0.15 Å, while the Al atoms in the second layer moved outward by 0.051 Å from their bulk positions. Meanwhile, the surface and subsurface N atoms moved outward by 0.035 and 0.020 Å, respectively. This feature is in agreement with the general description of a nonpolar semiconductor surface in which anions move outward and cations move inward. As a result of the inward displacement of surface Al atoms, the bond length between the Al on the first layer and N on the second layer changed by −1.32% to 1.87 Å. The Al-N bond lengths on the surface layer along $[1\bar{1}0\,0]$ and $[0\,0\,01]$ directions contracted by −4.4% (to 1.81 Å) and −5.7% (to 1.80 Å), respectively, from the corresponding bulk bond lengths. The relaxation of Al and N atoms in the subsurface layer is very small. The vertical buckling $\perp\Delta$ of the Al-N dimer on the surface layer is found to be 0.18 Å. Our results are in good agreement with previously reported Hartree-Fock-based calculations[16] on the $(11\bar{2}\,0)$ surface of an AlN slab and the local-density-approximation-based calculations on the surfaces of group-III nitrides.[17]

Figure 4(a) shows the total density of states (DOS) for spin-up and spin-down electrons of an undoped AlN $(11\bar{2}\,0)$ film, while Fig. 4(b) depicts the partial spin DOS corresponding to Al and N atoms. From the total DOS, we see that

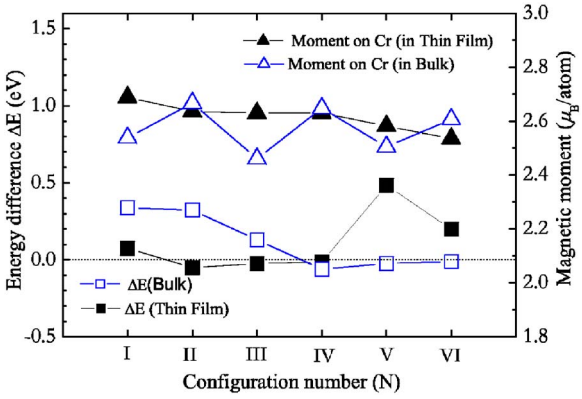

FIG. 3. (Color online) Magnetic moments and energy differences ΔE between AFM and FM states for the six configurations which are defined in the text for both bulk and thin film Cr-doped AlN. The unfilled triangle and circle are for the bulk $Al_{34}Cr_2N_{36}$ supercell, and the solid triangle and circle are for the thin film $Al_{68}Cr_4N_{72}$ supercell.

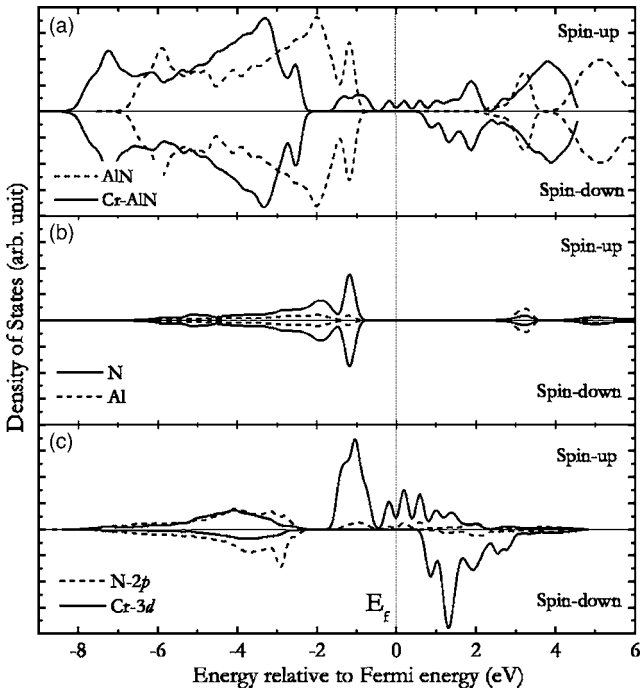

FIG. 4. (a) Total DOS corresponding to the undoped AlN $(11\bar{2}0)$ surface ($Al_{72}N_{72}$) (dashed line) and the Cr-doped one ($Al_{68}Cr_4N_{72}$) (solid line). (b) Partial spin DOS of Al $3p$ (dashed line) and N $2p$ (solid line). (c) Partial spin DOS of Cr $3d$ (solid line) and N $2p$ (dashed line) in $Al_{68}Cr_4N_{72}$.

the Fermi level is located in the gap region indicating the semiconducting nature of AlN thin films. The symmetric nature of spin-up and spin-down DOS curves also confirms the nonmagnetic nature of the $(11\bar{2}0)$ thin film.

We now present our results on Cr-doped AlN slabs. First we determine the preferred site of a single Cr atom. This was achieved by replacing Al on the surface (site no. 3) and subsurface layer (site no. 11) with Cr atoms successively, in Fig. 1. To preserve the symmetry of the supercell, the corresponding sites (site no. 65 or no. 58) on the bottom surface of the slab were successively replaced with Cr. The geometry optimization and the total energy calculation of these two configurations showed that the Cr atom has a very clear preference for surface site over subsurface site. The relaxed Cr-N bond lengths along $[1\bar{1}00]$ and $[0001]$ directions, in the ground state, are found to be 1.86 and 1.85 Å, respectively. The configuration in which the Cr atom is occupying the surface site is 2.61 eV lower in energy than the configuration with Cr occupying the subsurface site. The large energy difference between the two configurations can be attributed to the number of Al-N bonds that are broken as a result of Cr substitution in the surface and subsurface layer. Note that AlN is an ionically bonded system with a cohesive energy of 11.54 eV.[18] This corresponds to 2.89 eV/per Al-N bond. When an Al atom is replaced by Cr atom in the second layer, four Al-N bonds are broken, whereas in the case of Cr replacing Al on the surface layer, only three Al-N bonds are broken. The large energy difference (2.61 eV) between the surface and subsurface sites is close to the Al-N bond energy of 2.89 eV. Therefore, the substitutional doping of Cr in AlN thin film shows strong surface site preference. This site preference of the doped Cr atom is consistent with recently found trend in (Ga,Cr)N (Ref. 13) and (Zn,Cr)O (Ref. 19) thin films. In the Cr-doped GaN thin film, the surface substituted site is 1.55 eV lower in energy than that in the subsurface site, while in (Zn,Cr)O, it is about 0.59 eV lower in energy. The magnetic moment on each of the Cr atom on the surface and subsurface sites is around $2.64\mu_B$. This suggests that the magnetic moment at Cr is not sensitive to its environment. We will show that the magnetic coupling between the Cr atoms, however, depends upon the distance between them.

The magnetic coupling between the Cr atoms is studied by replacing two Al atoms with two Cr atoms on the surface and/or subsurface layers. To preserve symmetry we also replaced identical Al atoms with Cr atoms at the bottom of the slab. Hence, a total replacement of four Al with four Cr atoms results in 5.56% doping concentration and an $Al_{68}Cr_4N_{72}$ supercell. In this case, Cr atoms have a wide variety of choices on where it can replace the Al atoms. Two Cr atoms can replace two nearest-neighbor or two second-nearest-neighbor Al atoms on the surface layer or both the Cr atoms can occupy nearest-neighbor sites on the subsurface layer. Cr atoms can also replace two Al atoms, one on the surface layer and the other on the subsurface layer of the slab. So, in this study we have considered six different configurations. Configuration I represents the replacement of the nearest-neighbor Al atoms with Cr atoms, namely, nos. 3 and 8 on the surface layer and the corresponding symmetrically identical Al atoms at sites no. 65 and no. 71 on the bottom layer, identified in Fig. 1. In configuration II, we have replaced Al atoms on sites no. 3 and no. 6 on the surface layer, and nos. 65 and 68 in the bottom layer with Cr atoms. Configuration III corresponds to the replacement of Al atoms at sites nos. (3,4) and nos. (65,66) (see Fig. 1) with Cr atoms on either side of the slab. Configuration IV is achieved by replacing the farthest of the Al atoms, namely, Al on sites nos. (6,8) on the surface layer and nos. (68,71) on the bottom layer. Configuration V is achieved by replacing one Al atom on the surface layer and the other on the second layer with Cr atoms [nos. (3,13) and nos. (65,62) in Fig. 1]. Configuration VI corresponds to the replacement of nearest-neighbor Al atoms in the subsurface layer [nos. (11,13) and nos. (58,62)] of the slab with Cr atoms. It is to be noted here that the distance between the doped Cr atoms is different in each of these configurations, with the minimum initial distance being 3.07 Å in configuration I. Geometry optimization and total energy calculations were carried out on all these six configurations. Both FM and AFM states for each of these configurations were taken into consideration to identify the most preferred magnetic state and also to understand how the magnetic coupling between the Cr atoms vary with the distance between them. The optimized Cr-Cr distances and the nearest Cr-N bond lengths, the energy difference (ΔE), and the relative energies ($\Delta\epsilon$) with respect to the ground-state energy are collected in Table II.

Configuration I, with FM coupling between the Cr atoms occupying the nearest-neighbor sites on the surface layer, is found to be the lowest in energy than all the other configurations. The corresponding AFM state of configuration I is

TABLE II. The energy difference ΔE_0 (ΔE) between AFM and FM states ($\Delta E = E_{AFM} - E_{FM}$, in eV), the relative energy $\Delta\epsilon_0$ ($\Delta\epsilon$) (in eV) calculated with respect to the ground-state configuration I without (with) geometry optimization, and the optimized nearest Cr-N and Cr-Cr distances (in Å) for the thin film $Al_{68}Cr_4N_{72}$ supercell. First column identifies the Al sites in Fig. 1 that are replaced by Cr.

Configurations	ΔE_0	$\Delta\varepsilon_0$	ΔE	$\Delta\varepsilon$	Coupling	$d_{Cr\text{-}N}$	d_{Cr}-Cr
I (3, 8/65, 71)	0.087	0.000	0.075	0.000	FM	1.851	2.974
II (3, 6/65, 68)	−0.044	0.324	−0.050	0.384	AFM	1.892	4.444
III (3, 4/65, 66)	−0.008	0.309	−0.023	0.435	AFM	1.855	4.982
IV (6, 8/68, 71)	−0.002	0.261	−0.015	0.385	AFM	1.851	5.393
V (3, 13/65, 62)	0.241	2.873	0.494	2.110	FM	1.858	2.963
VI(11, 3/58, 62)	0.143	5.699	0.199	5.034	FM	1.940	2.990

0.075 eV higher in energy than the FM ground state. So our theoretical calculations verify the ferromagnetism in Cr-doped AlN thin film at very low doping concentrations, as reported in the experiments.[1–5] In the configurations with Cr atoms occupying various surface sites (configurations II–IV), the AFM state is lower in energy than their corresponding FM states. From Table II it is clearly seen that as the distance between the Cr atoms on the surface layer increases the energy differences between the AFM and FM states becomes smaller and the AFM state is slightly preferred over the FM state. The configurations in which Cr atoms are in the subsurface layers (configurations V and VI) do prefer FM coupling; however, their energies are high, namely, 2.11 and 5.03 eV higher than configuration I, respectively. These large energy differences with respect to the ground state can also be understood from the viewpoint of strong Al-N bond and the different number of Al-N bonds broken to reach configurations V and VI.

In the ground state, the Cr-N bond lengths on the surface layer are calculated to be 1.85 Å along $[1\bar{1}00]$ and 1.86 Å along [0001] directions. The surface relaxation has resulted in a shortening of Cr-Cr bond length, from 3.07 to 2.97 Å. The preference for configuration I as the ground state clearly indicates that the doped Cr atoms not only prefer to occupy the surface sites, but also prefer to cluster around the N atoms. This is in agreement with the recent studies of Cr-doped GaN.[20,13] In the ground state, the doped Cr atoms are ferromagnetically coupled, with a magnetic moment of $2.68\mu_B$ on each of them. A majority contribution of this magnetic moment comes from its $3d$ orbital ($2.62\mu_B$). Meanwhile, the neighboring N atom is polarized antiferromagntically by the Cr atom, carrying a magnetic moment of $-0.11\mu_B$. The magnetic moments located on each Cr atom for all the configurations are plotted in Fig. 3. Note that Cr atom carries a magnetic moment ranging from$2.535\mu_B$ to $2.688\mu_B$. In previously reported experiments,[1–3,5,6] the magnetic moments on the Cr atom varied with the method of synthesis of the AlN thin film and also with the possibility of disorder in the film. In a recently reported experiment on Cr-doped AlN thin film,[1] the maximum magnetic moment on the Cr atom of $0.71\mu_B$ at 50 K was achieved at a 2.7% doping concentration. In another experimental study,[6] it was reported that only 10% of the doped Cr contributed to the ferromagnetism in the sample. This reduced net magnetic moment and low percentage of Cr atoms contributing toward ferromagnetism can arise if all the Cr atoms are unable to form nearest neighbors even though energetically this is the most preferred configuration. For those Cr atoms that are at larger distances from each other due to barriers against diffusion, the coupling will be AFM (as seen in our theoretical calculations) and so those Cr atoms cannot contribute to the observed saturation magnetic moment of the sample. Thus the observed value will be reduced. So, we can conclude that the upper limit of the magnetic moment of the Cr atom is $2.68\mu_B$.

The total DOS of undoped and Cr-doped AlN for the ground-state configuration, along with the partial spin DOS of Al $3p$ and N $2p$ are given in Figs. 4(a) and 4(b), respectively. The partial spin DOSs of Cr $3d$ and N $2p$ are shown in Fig. 4(c). From Fig. 4(a), it is clearly seen that the doping of Cr in the AlN thin film has introduced new states in the energy gap resulting in a half-metallic character of the doped system. Meanwhile, Fig. 4(c) shows that the Cr $3d$ levels dominate the density of states at the Fermi energy with an overlap between the N $2p$ and Cr $3d$ states. This shows that there is a strong interaction between Cr and the nearing N atoms, which results in the opposite magnetic moments of N atoms, similar to what happens in Cr_2O and Cr_2N molecules.[21,22]

In Fig. 5(a) we present the charge density distribution in the surface layer of a pure AlN thin film and compare it with those when one and two Cr atoms are substituted on the surface layer. Note that there is very little overlap between charge densities on Al and N sites in pure AlN indicating the bonding to be ionic. However, when a Cr atom is substituted at the Al site, charges between Cr and nearest N sites do overlap and this overlap drives the coupling to be FM.

To explore the effect of Coulomb correlation on the magnetic coupling of the Cr-doped AlN thin film, we have employed the local spin density approximation $+U$ method.[23,24] We considered the Coulomb correction for Cr $3d$ electrons for the ground-state configuration I (3, 8/65,71) of the $Al_{68}Cr_4N_{72}$ supercell for both FM and AFM spin alignments. In this method, the Coulomb interaction among the localized electrons (e.g., transition metal d) has been replaced by statically screened parameters U and J. We chose $J=0.87$ eV and $U=3$ eV which were used in some previous calculations.[25,26] It was found that the FM coupling is energetically still more favorable, with the FM state lying 0.114 eV lower in energy that the AFM state. The value of the local magnetic moment

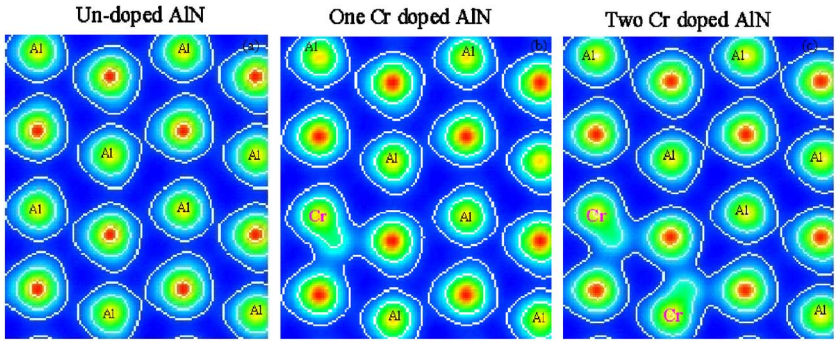

FIG. 5. (Color online) Charge density distribution of (a) $Al_{72}N_{72}$, (b) $Al_{70}Cr_2N_{72}$, and (c) $Al_{68}Cr_4N_{72}$ in the plane of the surface layer.

at the Cr site increases from $2.681\mu_B$ to $2.920\mu_B$. It is important to note that the introduction of U does not change the magnetic coupling between Cr atoms in an AlN thin film. This further confirms the stability of the FM coupling in Cr-doped AlN thin films. The mechanism driving this FM coupling is found to be similar to that in Cr-doped GaN thin films,[13] namely, it is mediated by the hybridization of Cr $3d$ and N $2p$ orbitals and hence is driven by double exchange.

IV. SUMMARY

The site preference and magnetic coupling of Cr atoms doped in AlN bulk and thin films are studied extensively within the framework of density functional theory. It is found that in both bulk and thin films, Cr atoms prefer to cluster around N and ferromagnetic coupling is energetically more stable. However, in the case of thin film, due to the high energy cost for breaking the strong Al-N bonds, Cr atoms prefer to reside on the surface sites. Our theoretical results are in agreement with the recent experimental observations where ferromagnetism in Cr-doped AlN thin films has been reported. The calculated magnetic moment, however, is significantly larger than the experimental result. In a recent paper[20] Cui *et al.* have shown that in Cr-doped GaN, Cr atoms, in a supercell containing three or more Cr, prefer to cluster and the coupling between them become *ferrimagnetic*, thus resulting in partial cancellation of moments. This would explain the observed low magnetic moment per Cr atom. However, in our calculation, we have used a low concentration of Cr atoms. To study the effect of Cr clustering in AlN thin films where the Cr concentration is the same as that used here, a much larger supercell is needed. We are presently studying this problem and the results will be published in due course.

We have also shown that the ferromagnetic coupling between Cr atoms in the AlN thin film is short-range. It is legitimate to wonder how the short-ranged ferromagnetism can be reconciled with the existence of high Curie temperature in a diluted system. Note that the computation of the Curie temperature using first-principles method is difficult and the common practice of using phenomenological models lacks quantitative accuracy. However, the Curie temperature can be enhanced by strong coupling between neighboring magnetic ions as well as by coupling between the magnetic ions between adjoining supercells. In the former the energy difference between the FM and AFM states provides an indication of the strength of magnetic coupling. For the latter, calculations are necessary by doubling the size of the supercell. This is computer intensive and will be attempted at a later time. However, we should point out that in two recent calculations[27,28] the magnetic coupling in dilute magnetic semiconductors has been demonstrated to be dominated by short-ranged interatomic interactions and it was shown that the magnetic ordering is heavily influenced by magnetic percolation.

ACKNOWLEDGMENTS

The work was supported in part by a grant from the Office of Naval Research. The authors thank Y. Kawazoe and the staff of the Center for Computational Materials Science, the Institute for Materials Research, Tohoku University (Japan), for their continuous support of the HITACH SR8000 supercomputing facility.

[1] D. Kumar, J. Antifakos, M. G. Blamire, and Z. H. Barber, Appl. Phys. Lett. **84**, 5004 (2004).
[2] S. Y. Wu, H. X. Liu, L. Gu, R. K. Singh, L. Budd, M. van Schilfgaarde, M. R. McCartney, D. J. Smith, and N. Newman, Appl. Phys. Lett. **82**, 3047 (2003).
[3] R. M. Fraizer, J. Stapleton, G. T. Thaler, C. R. Abernathy, S. J. Pearton, R. Rairigh, J. Kelly, A. F. Hebard, M. L. Nakarmi, K. B. Nam, H. X. Jiang, J. M. Zavada, and R. G. Wilson, J. Appl. Phys. **94**, 1592 (2003).
[4] S. G. Yang, A. B. Pakhomov, S. T. Hung, and C. Y. Wong, Appl. Phys. Lett. **81**, 2418 (2002).
[5] H. X. Liu, S. Y. Wu, R. K. Singh, L. Gu, N. R. Dilley, L. Montes, and M. B. Simmonds, Appl. Phys. Lett. **85**, 4076 (2004).
[6] A. Y. Polyakov, N. B. Smirnov, A. V. Govorkov, R. M. Fraizer, J. Y. Liefer, G. T. Thaler, C. R. Abernathy, S. J. Pearton, and J. M. Zavada, Appl. Phys. Lett. **85**, 4067 (2004).
[7] M. van Schilfgaarde and O. N. Mryasov, Phys. Rev. B **63**, 233205 (2001).
[8] Y. Wang and J. P. Perdew, Phys. Rev. B **44**, 13298 (1991).
[9] G. Kresse and D. Joubert, Phys. Rev. B **59**, 1758 (1999).

[10] P. E. Blochl, Phys. Rev. B **50**, 17953 (1994).
[11] G. Kresse and J. Furthmüller, Phys. Rev. B **54**, 11169 (1996).
[12] H. J. Monkhorst and J. D. Pack, Phys. Rev. B **13**, 5188 (1976).
[13] Q. Wang, Q. Sun, P. Jena, J. Z. Yu, R. Note, and Y. Kawazoe, Phys. Rev. B **72**, 045435 (2005).
[14] Q. Wang, Q. Sun, P. Jena, and Y. Kawazoe, Nano Lett. **5**, 1587 (2005).
[15] G. P. Das, B. K. Rao, and P. Jena, Phys. Rev. B **69**, 214422 (2004).
[16] K. Kádas, S. Alvarez, E. Ruiz, and P. Alemany, Phys. Rev. B **53**, 4933 (1996).
[17] U. Grossner, J. Furthmüller, and F. Bechstedt, Phys. Rev. B **58**, R1722 (1998).
[18] W. A. Harrison, *Electronic Structure and the Properties of Solids* (Dover, New York, 1989), p. 176.
[19] Q. Wang, Q. Sun, P. Jena, and Y. Kawazoe, Appl. Phys. Lett. **87**, 162509 (2005).
[20] X. Y. Cui, J. E. Medvedeva, B. Delley, A. J. Freeman, N. Newman, and C. Stampfl, Phys. Rev. Lett. **95**, 256404 (2005).
[21] K. Tono, A. Terasaki, T. Ohta, and T. Kondow, Phys. Rev. Lett. **90**, 133402 (2003).
[22] Q. Wang, Q. Sun, B. K. Rao, P. Jena, and Y. Kawazoe, J. Chem. Phys. **119**, 7124 (2003).
[23] V. I. Anisimov, J. Zaanen, and O. K. Andersen, Phys. Rev. B **44**, 943 (1991).
[24] A. I. Liechtenstein, V. I. Anisimov, and J. Zaanen, Phys. Rev. B **52**, R5467 (1995).
[25] M. A. Korotin, V. I. Anisimov, D. I. Khomskii, and G. A. Sawatzky, Phys. Rev. Lett. **80**, 4305 (1998).
[26] T. Tsujioka, T. Mizokawa, J. Okamoto, A. Fujimori, M. Nohara, H. Takagi, K. Yamauva, and M. Takano, Phys. Rev. B **56**, R15509 (1997).
[27] L. Bergqvist, O. Eriksson, J. Kudrnovsky, V. Drchal, P. Korzhavyi, and I. Turek, Phys. Rev. Lett. **93**, 137202 (2004).
[28] K. Sato, W. Schweika, P. H. Dederichs, and H. Katayama-Yoshida, Phys. Rev. B **70**, 201202(R) (2004).